10-1975

Response of Saturated Sands to Cyclic Shear at Earthquake Amplitudes

Vincent P. Drnevich
University of Kentucky

John P. Jent
University of Kentucky

Research Report No. 87

RESPONSE OF SATURATED SANDS TO CYCLIC SHEAR AT EARTHQUAKE AMPLITUDES

by

Dr. Vincent P. Drnevich
Principal Investigator

and

John P. Jent
Graduate Assistant

October, 1975

ABSTRACT

Both quasi-static and resonant cyclic shear tests were performed on hollow cylindrical specimens of saturated sands at various densities and confining stresses. Shear moduli measured at nondestructive amplitudes were shown to be independent of frequency for the range of 0.1Hz to 50Hz. Application of cyclic shear at larger amplitudes caused effective stresses to decrease and failure. The number of cycles to failure was related to ratio of cyclic shear stress to maximum drained shear stress. Effective confining stress reduces approximately linearly with number of cycles. Shear modulus and shear damping can be described by the Hardin-Drnevich equations if change in effective stress is properly adjusted. Procedures were developed to use research results in analyzing soil in dam or other profiles to predict factor of safety against liquefaction failure and to estimate shear modulus and damping of soils for subliquefaction conditions when these soils are subjected to earthquakes.

ACKNOWLEDGMENTS

TABLE OF CONTENTS

iv

LIST OF TABLES

v

LIST OF FIGURES

CHAPTER I

INTRODUCTION

Earthquakes cause cyclic compressive and shear stresses in soils. Shear stresses are by far the more important because they are responsible for the catastrophic failures that are recorded. When cyclic shear stresses are applied to a saturated sand soil and when the duration of application is short in relation to the time required for the pore water to drain from the sand, then the effect of the cyclic shear stress is to cause the pressures in the pore water to increase. Associated with this increase in porewater pressure is a decrease in effective stress and shear strength. The reduction in shear strength leads to shear failures and what is generally termed liquefaction.

The principal objective of this project is to define the change in effective confining pressure, shear modulus and shear damping in a variety of saturated sands for undrained conditions due to the application of cyclic shear. The range of shear strain amplitudes and frequencies applied to specimens in the laboratory simulate those associated with minor tremors through strong motion earthquakes.

CHAPTER II

RESEARCH PROCEDURES

The application of cyclic shear to soil specimens in the laboratory was achieved by use of a resonant column apparatus that was modified to perform quasi static as well as resonant tests. The apparatus is shown in Fig. 1. For the tests in this program, the apparatus applied cyclic torsion to the top of a hollow cylindrical soil specimen that was fixed at its bottom. The dimensions of the specimen were: 5 cm (1.97 inches) outside diameter, 4 cm (1.57 inches) inside diameter, and 10 cm (3.94 inches) length.

The reason for using a hollow cylindrical specimen was that for torsion, the shear stress and shear strain are relatively constant over the entire volume of the specimen. Furthermore, with this configuration there is no discontinuity of boundary conditions on vertical planes passing through the axis of the specimen. There are, however, horizontal boundary planes of discontinuity at the top and bottom of the specimen. Problems here are minimized by grooving the portion of the platens that make contact with the specimen.

The specimens were formed using a mandrel to maintain the inside diameter and a mold to maintain the outside diameter. The mandrel had a 0.030 cm (0.012 inch) thick membrane pulled over it and the mold was lined with a second membrane that was held to the mold by means of a vacuum. Details of the equipment associated with specimen construction are given in a report by Jent (7).

Sand was then placed in the annular space between the inner and outer membranes. The method of placement varied depending on the sand being tested and on the desired density. The procedures used ranged from simply spooning the sand into the mold, to raining it through a tube from various heights above the mold, to allowing it to settle to the bottom of a water filled mold. This last method gave very loose specimens but was only used for soils that were composed of practically one sized particles. An alternate method for obtaining

2
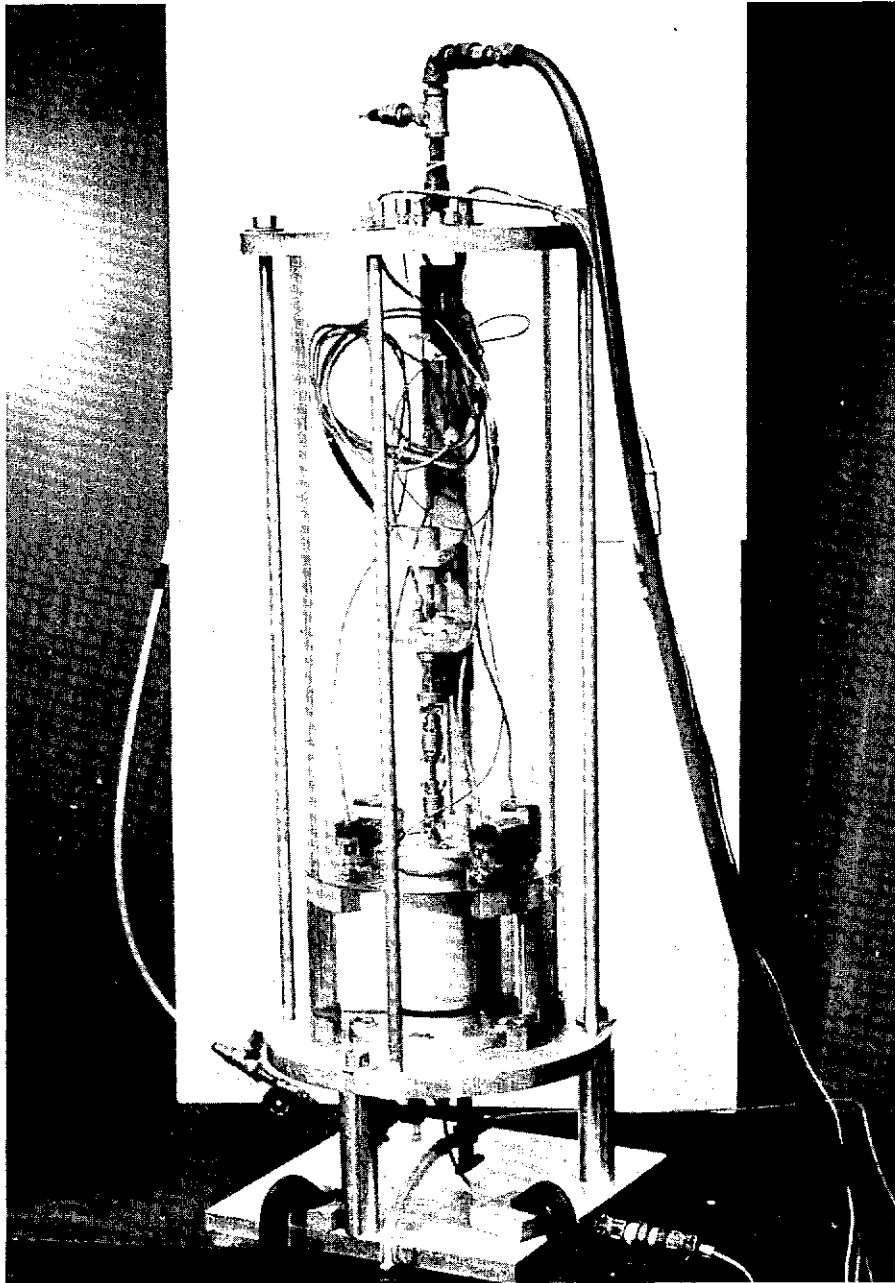
Fig. 1 Cyclic Shear Test Apparatus

loose specimens was to "bulk" the sand by mixing in small amounts of water and then placing the sand into the mold. With the mold partially filled, water was very slowly introduced to the specimen through holes in the lower platen. The water was then drained from the specimen, additional bulked sand was added and the process repeated until the annular space between the mold and the mandrel was filled with the sand.

Specimen construction was completed by placing the top platen on the specimen and sealing the inner and outer membranes to the top platen.

Before the mandrel and mold could be removed, a vacuum was applied to the interior of the specimen through the hole in the lower platen. The vacuum provided sufficient confinement to the specimen that the mandrel and mold could be removed, specimen dimensions could be measured, and the torsional loading plate could be fastened to the upper platen. A completed specimen is shown in Fig. 2.

The torsional loading portion of the apparatus consisted of an electromagnetic torque motor formed by four stationary coils placed in the gaps of four permanent magnets that were attached. A view of this torque motor is given in Fig. 3.

The final step in preparing the apparatus was to enclose the entire specimen--torque motor system with a pressure chamber consisting of a clear cast acrylic tube and lid as shown in Fig. 1. To reduce infiltration of air into the specimen, water was introduced into the chamber to completely cover the specimen. Thus, an air-water interface existed just below the torque motor. The air in the pressure chamber was pressurized by means of a regulated compressed air supply.

The next stage in preparation was to saturate the specimen. With some positive pressure applied inside the chamber, the vacuum to the pore space was shut off and deaired distilled water was allowed to fill the evacuated pore space. This procedure was usually insufficient to completely saturate the specimen so that back pressuring was also needed. The process of back pressuring involves applying equal increments of pressure to both the chamber and the pore fluid. In this case, 4 bars (58 psi) back pressure was usually sufficient to ensure saturation. Saturation was checked by noting the pore water
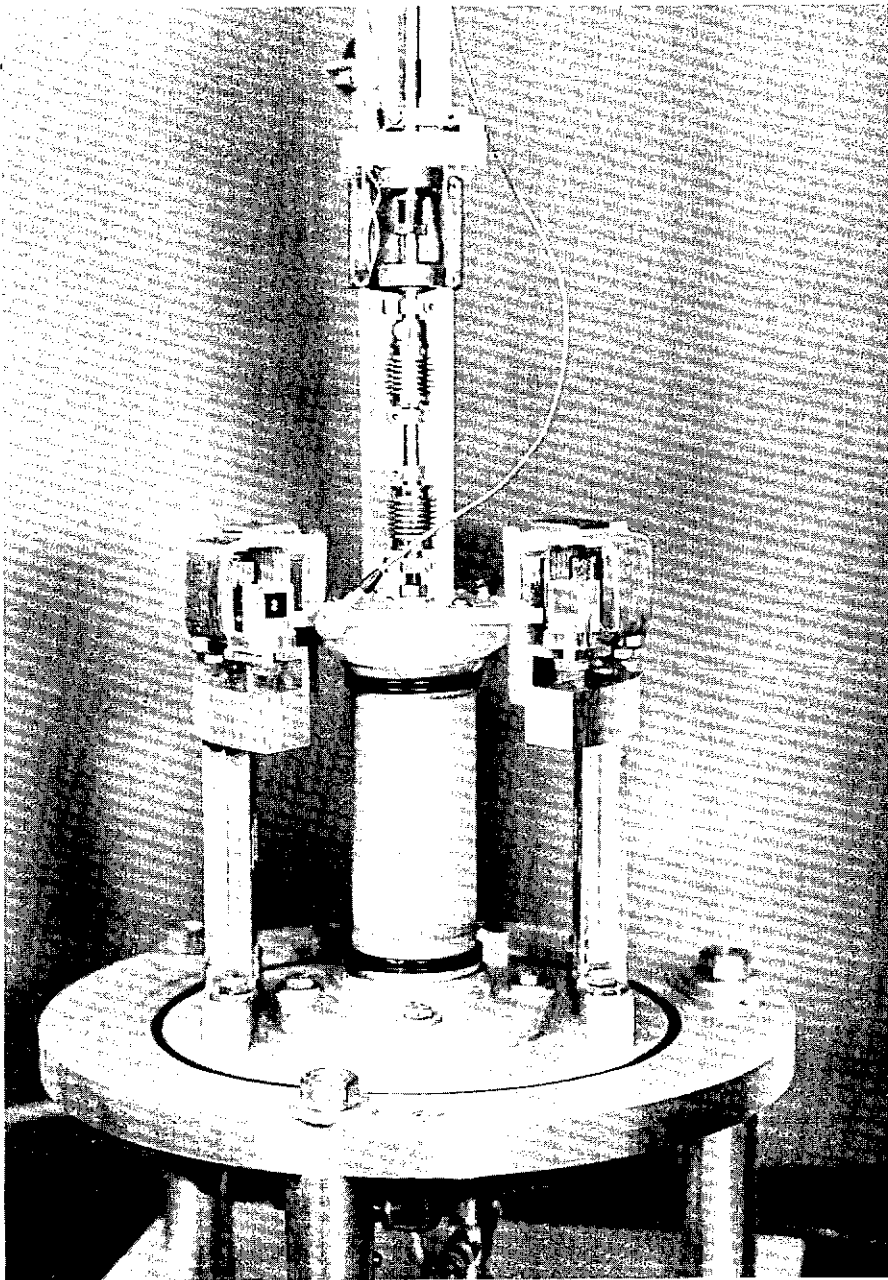
Fig. 2   Completed Test Specimen

5
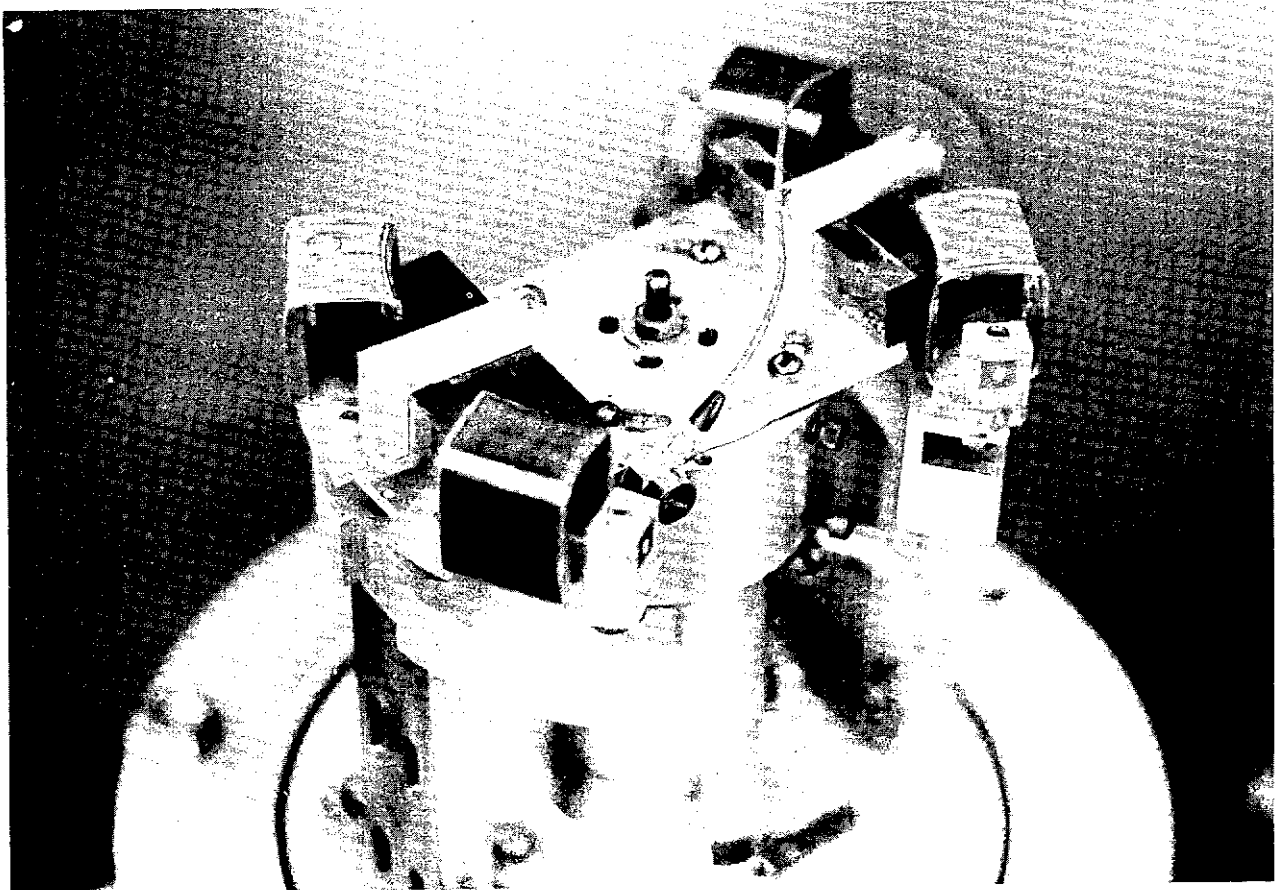
Fig. 3   Torque Motor of Apparatus

pressure increase with drainage valves closed for a given increase in chamber pressure. A specimen was considered saturated if the pore water pressure increase was 98% to 100% of the chamber pressure increase. This corresponds to Skempton B pore pressure coefficients of 0.98 to 1.00.

The torque motor and its accompanying electronics was capable of applying oscillating torques of controlled amplitudes at frequencies ranging from zero to several thousand cycles per second. Generally, only two ranges were used in this program, quasi-static and resonance. The quasi-static range included frequencies to one cycle per second. These were low enough that all inertia effects of the specimen and torque motor could be neglected and that both the torque and resulting rotational displacement could be plotted on a conventional X - Y pen recorder. The resulting plots consisted of hysteresis loops where the ordinate value was proportional to applied shearing stress and the abscissa was proportional to shearing strain in the specimen. Shear modulus was obtained from the slope of the hysteresis loop and damping from both the slope and the area enclosed by the loop. The procedures for these data reduction are given by Hardin and Drnevich (5). Calibrations gave the constants of proportionality for stress and strain. The loop areas were determined by use of a planimeter.

Testing at resonance involved applying the torque and adjusting the frequency until the first mode undamped natural frequency of the soil-torque motor system was achieved. By use of the polar mass moments of inertia of the specimen and of the torque motor, it was possible to calculate the shear modulus of the soil by use of wave propagation theory (2) (4). Likewise, the damping ratio determination was determined by the magnification factor method which is based on wave propagation theory (2).

Shear strain amplitudes in the specimen were related to the rotational amplitudes at the top of the specimen (the bottom of the specimen was fixed). For the quasi-static testing, a special transducer was constructed from two linearly varying differential transformers. This transducer had to be extremely sensitive to rotational motion and virtually independent of vertical or horizontal motion. A commercially available transducer and two made in-house transducers were tried without success until the third in-house transducer

7

proved satisfactory. Details of this transducer are given by Jent (7).

For resonance testing, the rotational motion was measured with
an accelerometer. Rotational motion was obtained by assuming
semisoidal motion and dividing the accelerometer output by $(2\pi f)^2$
where f is the frequency of vibration.

In essence, the quasi=static and resonance measuring systems
and methods of data reduction were independent of each other. As a
consequence, determination of modulus and damping at nondestructive
shear strain amplitudes (shear strains less than 2. x 10^{-5}) was done
by both quasi-static and resonance methods prior to the application of
any large amplitude cyclic stresses.

The main part of each test was the cyclic straining at large
amplitudes. For this portion of the test, the drainage line through the
lower platen was closed. The pore water pressures in the specimen
during this portion of the test were measured by a differential pore
pressure transducer mounted directly in the lower platen. The other
side of this pressure transducer was connected to the chamber pres-
sure and hence the output of the transducer gave cell pressure minus
pore pressure or effective confining stress. For quasi-static tests,
the effective stress was plotted as the abscissa and the shearing stress
as the ordinate on a second X - Y recorder. The resulting plot was
a stress path (8) for the undrained cyclic shearing portion of the test.
The output of the pressure transducer was also plotted on a strip chart
recorder so that a record of pressure with cycles of loading was also
made.

For resonance tests, the frequencies of cyclic shearing were
too large for the X - Y and strip chart recorders. The pressure
transducer output was displayed on a digital voltmeter and was manually
recorded.

The specimen also tends to change in length during cyclic straining.
A linearly varying differential transformer located above the torque
motor measured length changes in the specimen. The output of this
transducer was displayed on a digital voltmeter and for the quasi-
static tests was plotted on the second channel of the strip chart recorder.

The procedure for each test was as follows: 1) determine the
soil behavior at nondestructive strain amplitudes by both quasi-static

8

and resonance methods; 2) prevent drainage and apply large amplitude cyclic shear stresses at frequencies in the quasi-static range. 3) After 500 to 1000 cycles (or less if the effective stresses reduced to zero before that many cycles), determine the soil behavior at non-destructive strain amplitudes by both the quasi-static and resonance methods; 4) If the effective stresses were not near zero, use frequencies at resonance to apply cyclic shear stresses of approximately the same amplitude as those applied by the previous quasi static testing; 5) After the effective stresses reduced to near zero (whether or not step 4) above was done), the drainage valve was opened and the pore water allowed to flow from the specimen and the effective stress increase back to its original value. The volume of pore water expelled and any length changes were also recorded; 6) The soil behavior after testing was again measured by both quasi-static and resonance methods at nondestructive strain amplitudes; and 7) In a number of tests, steps 2) through 6) were repeated once or twice on the same specimen.

The above steps indicate that a tremendous quantity of data were generated for each test. These data were cataloged and were put on punched cards after each test. Computer codes were used to reduce the data and to give a punched deck as well as a listing of the reduced data. Most data analysis and plotting were accomplished by use of the University of Kentucky's digital computer and Calcomp plotter.

CHAPTER III

DATA AND RESULTS

In the research program, forty-six tests were run. Five different sands were tested. To make the results more useful for other sands, specific gravity, particle size distribution and relative density tests were run on the five sands. The results of these tests are given in Table I and the particle size distribution curves are given in Fig. 4. The maximum and minimum densities for the sands were determined by use of ASTM Standard No. 2049-69 with one deviation. The size of the specimen container was 220 cm^3 (0.0078 cu. ft.) instead of the specified 2832. cm^3 (0.10 cu. ft.) container. Since the largest particle size of the soils tested was less than 1. mm (0.04 inch), which was less than 1/50th of the container diameter, it was felt that the results would be unaffected by container size. A review of the results indeed confirmed that they were consistent with what would be expected for these sands.

After each specimen was constructed, its dimensions were measured to establish the initial volume and void ratios. Then each specimen was saturated by means of back pressuring to 4.0 Kg/cm^2. The effective stress was maintained at 0.5 Kg/cm^2 during the back pressuring process. After back pressuring, the desired effective confining stress was applied by adjusting the cell pressure. Consolidation occured almost instantly. Before closing the drainage lines and the undrained cyclic shearing, both quasi-static and resonant cyclic shear cycles at extremely small strain amplitudes (less than 0.2 x 10^{-4} Rad) were applied to the specimen to establish the initial tangent shear modulus and damping. Results of these tests and other initial conditions are tabulated in Table II for all tests in the program.

Values of confining pressure, σ_o', are in terms of effective stress. The values in Table II were obtained from the difference between the cell pressure and the back pressure and with a correction stress of 0.02 Kg/cm^2 added to

Table I Conventional Characteristics of Test Program Sands

Name	Description	Specific Gravity	Uniformity Coefficient	Coefficient of Concavity	Unified Class.	Min Density (g/cm^3)	Max Density (g/cm^3)
Ottawa Sand (40-60)	white, uniform subrounded silica sand	2.66	1.31	.95	SP	1.38	1.65
Reid Bedford Model Sand	white, tan, & brown particles, subrounded	2.65	1.79	1.14	SP	1.46	1.75
Hawaii Beach Sand	white, subrounded to subangular silica sand	2.66 (Est.)	2.06	.89	SP	1.45	1.70
Monterey Beach Sand	tan subrounded sand	2.65	2.27	.99	SP	1.47	1.73
Granite Sand	tan subangular sand with silty fines	2.72	5.29	1.11	SM-SP	1.17	1.56

11
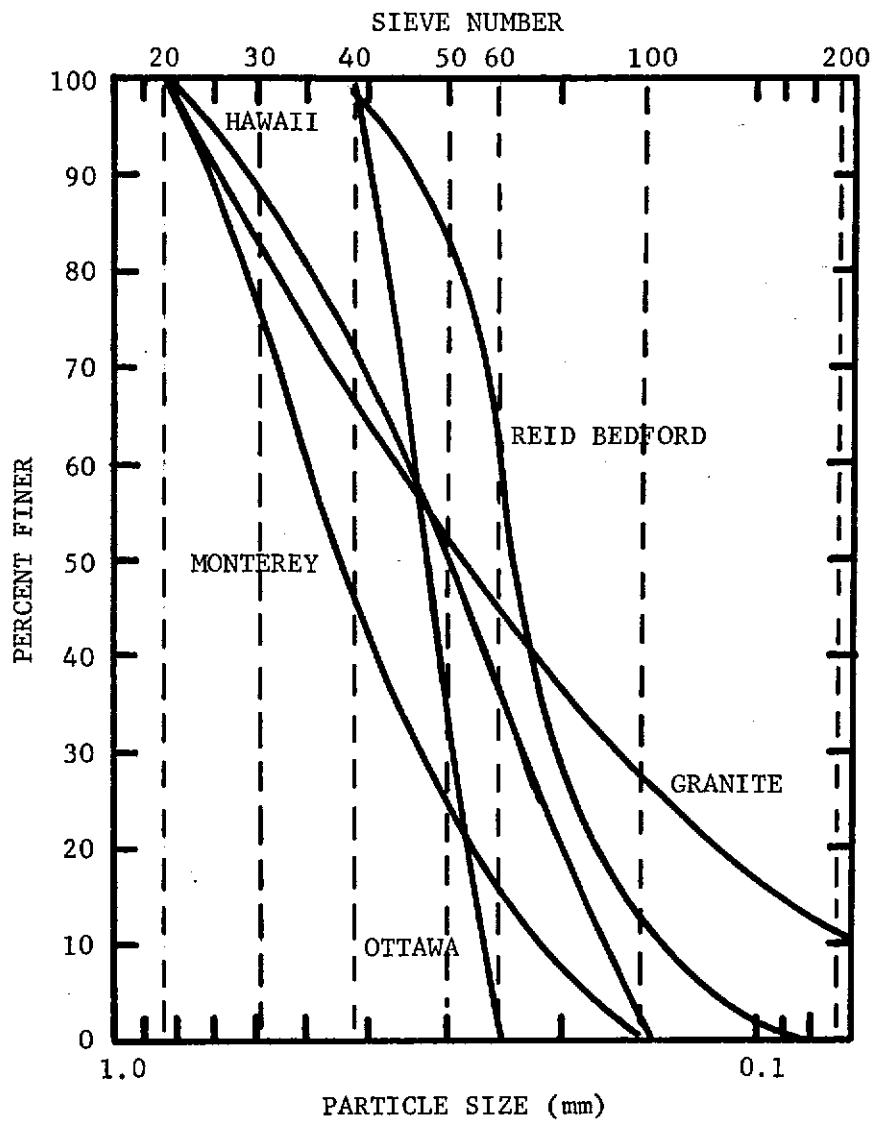
Fig. 4 Particle Size Distribution Curves for Soils in Testing Program

Table II Initial Conditions for Soils Tested

Test No.	Soil Name	Void Ratio	Rel. Density (%)	Cont. Press. (K_g/cm^2)	τ_{max} (K_g/cm^2)	$(G_{max})_{QS}$ (K_g/cm^2)	$(G_{max})_R$ (K_g/cm^2)	$(Damp)_R$ (%)
1	Ottawa	0.74	60	1.02	0.614	878.	900.	2.15
2	"	0.70	72	1.02	0.639	---	932.	2.50
3	"	0.68	78	0.52	0.332	---	615.	1.49
4	"	0.64	91	1.02	0.677	660.	942.	1.40
5	"	0.65	88	0.52	0.343	703.	622.	3.80
6	"	0.69	75	0.27	0.171	---	423.	4.02
7	"	0.70	72	0.52	0.326	---	718.	4.08
8	"	0.65	88	1.02	0.672	1059.	955.	2.86
9	"	0.64	91	0.27	0.179	447.	487.	1.42
10	"	0.66	84	1.02	0.664	---	981.	3.09
11	"	0.68	78	0.52	0.332	---	671.	1.51
12	"	0.86	20	0.52	0.268	554.	424.	3.40
13	"	0.75	55	0.52	0.307	804.	559.	3.22
14	"	0.81	35	0.52	0.285	545.	488.	2.63
15	"	0.78	47	1.02	0.585	998.	765.	3.59
16	"	0.80	40	0.27	0.151	435.	453.	3.89
17	"	0.81	37	0.27	0.149	340.	340.	1.77
18	"	0.79	42	0.27	0.152	313.	375.	4.26
19	"	0.80	40	2.02	1.129	900.	1075.	2.56
20	"	0.76	54	0.52	0.306	698.	577.	5.26
21	Reid Bed.	0.73	28	0.52	0.277	556.	474.	2.36
22	" "	0.74	23	0.52	0.271	495.	528.	2.43
23	" "	0.72	31	0.52	0.280	617.	607.	2.26
24	" "	0.74	23	1.02	0.531	791.	740.	1.53
25	" "	0.73	27	1.02	0.541	556.	828.	2.15
26	" "	0.72	31	1.02	.550	663.	810.	2.29

Table II, Cont'd. Initial Conditions for Soils Tested

Test No.	Soil Name	Void Ratio	Rel. Density (%)	Cont. Press. (K_g/cm^2)	τ_{max} (K_g/cm^2)	$(G_{max})_{QS}$ (K_g/cm^2)	$(G_{max})_R$ (K_g/cm^2)	$(Damp)_R$ (%)
27	Reid Bed.	0.72	31	1.02	.550	661.	747.	1.79
28	" "	0.74	22	1.02	.530	694.	731.	1.55
29	" "	0.69	40	1.02	.570	618.	792.	3.74
30	" "	0.63	58	1.02	.610	810.	980.	2.60
31	" "	0.65	52	1.02	.597	825.	896.	1.51
32	Monterey	0.57	87	0.52	.341	---	742.	.65
33	"	0.67	50	0.52	.302	708.	672.	.88
34	"	0.69	43	0.52	.294	860.	705.	.71
35	"	0.66	51	0.52	.303	918.	746.	.94
36	"	0.65	58	1.02	.610	1310.	1024.	.69
37	"	0.62	68	0.52	.322	628.	751.	.92
38	Granite	0.89	74	0.22	.139	---	133.	2.96
39	Hawaii	0.67	62	0.52	.315	669.	574.	.68
40	"	0.66	65	0.52	.318	---	---	---
41	"	0.67	63	0.52	.316	617.	594.	.65
42	"	0.67	60	0.52	.313	611.	603.	.56
43	"	0.65	68	0.52	.322	665.	594.	.56

14

account for water in the cell and membrane stresses.

The shear strength, τmax, was calculated from

$$\tau_{max} = \sigma_o' \sin \phi'$$

where σ_o' is the mean effective stress, and

ϕ' is the effective angle of shearing resistance which was estimated from the Meyerhof(9) equation $\phi = 28^o + 0.15$ (Rel. Density)

Initial tangent shear moduli were determined by two independent methods. Those determined by quasi-static testing are denoted by subscript "QS" and those determined by resonance testing are denoted by subscript "R". Since these values were determined at vastly different frequencies (0.1 Hz as opposed to 30 Hz to 50 Hz) and because they were determined with independent systems, it is instructive to compare their results. This is done in Fig. 5 where the quasi-statically determined values are plotted on the ordinate. Data scatter is relatively high but on the average, the two methods give the same moduli. The source of the data scatter was primarily in the quasi-static results. This can be verified by comparing the values obtained from resonance tests with values predicted by the Hardin equation (6) which is done in Fig. 6 where there is much less data scatter. Furthermore, the determination of initial tangent modulus by quasi-static testing is very sensitive to even the slightest friction in the apparatus.

The damping values listed in Table II were obtained by resonance testing. It was impossible to obtain any values from the quasi-static testing because for such low values, the area of the hysteresis loops are too small to be accurately determined with a planimeter. In general, these damping values should be small. The irregularity in values is due to varying amounts of apparatus friction that existed.

The last item in Table II is the reference strain. This parameter is defined as τ_{max}/G_{max} and was first used by Hardin and Drnevich (6) as means of normalizing shear strain data from a variety of soils and ambient conditions. It was also used by Drnevich (3) as a means of describing soil behavior due to undrained cyclic shear.

Once the initial information was determined on each specimen, the pore water drainage valve was closed and quasi-static cyclic shear stresses were
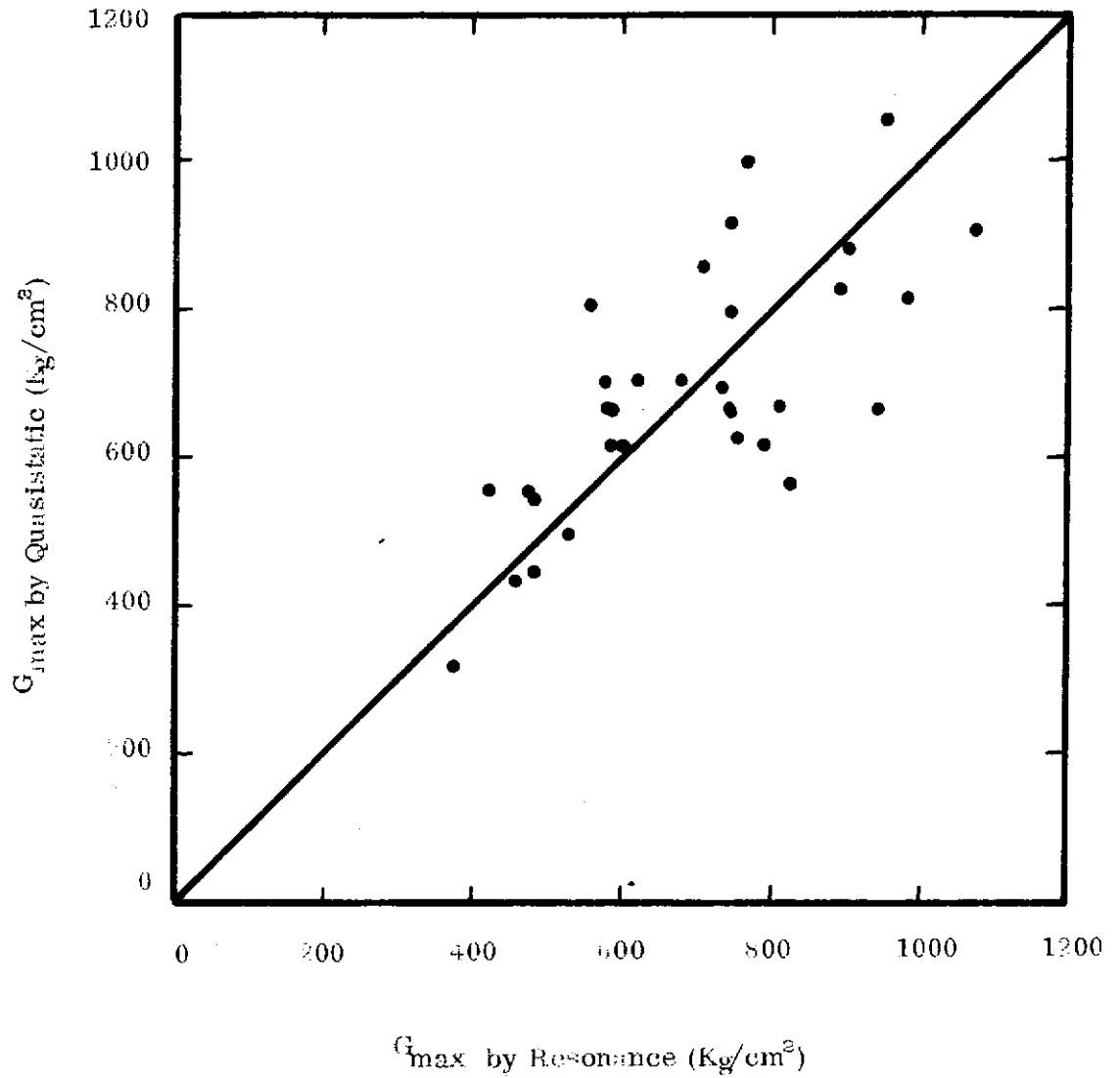
Fig. 5 Comparison of G_{max} from Quasi-static and Resonance Tests
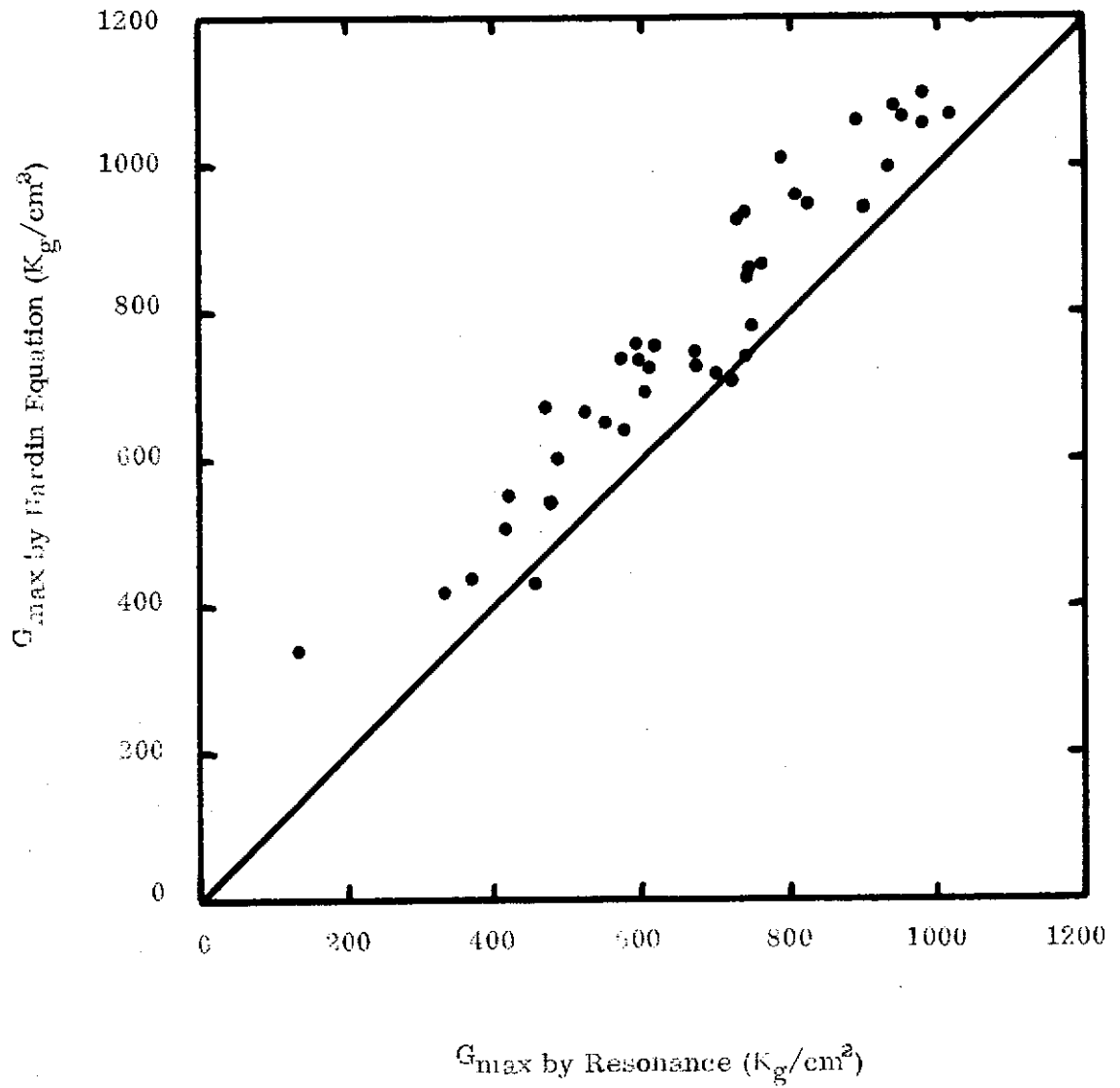
Fig. 6 Comparison of G_{max} from Resonance Tests with Values Calculated by Hardin Equation

applied. The data were recorded on two x-y recorders and one strip chart recorder. The first x-y recorder displayed the applied torque versus the rotational deformation of top of the specimen. Assuming that the torque is proportional to shear stress and that the rotation is proportional to shear strain, the resulting hysteresis loops (see example in Fig. 7a) can be considered stress-strain curves. The equivalent elastic shear modulus for any cycle was determined from the slope of a line that connects the end points of the loop. The shear damping associated with a given cycle was determined from the area of loop according to the procedure discussed by Hardin and Drnevich (5).

The other x-y recorder displayed the torque as the ordinate versus the mean effective confining stress as the abscissa. The mean effective confining stress was measured by means of a differential pressure transducer with one side connected to the chamber pressure and the other side connected to the pore water pressure. The resulting curves (see Fig. 7b for an example) were plots of the effective stress paths due to the undrained cyclic shear. The plot starts at the right and with undrained cyclic shear moves to the left denoting a reduction in the effective confining stress. As failure begins, the loading portion curves tend to bend to the right denoting that dilation is taking place.

The results of the testing program are outlined in Table III. The ratio τ/τ_{max} was the value of applied shear stress divided by the maximum shear stress possible for the confining stress at the start of the test. These two parameters are shown in Fig. 8 which is a plot of stress paths. If the cyclic shear were applied with drained conditions, the first 1/4 cycle of loading would have the stress path denoted by the vertical vector labelled τ. The maximum shear stress for this condition would be the vertical vector, τ_{max}, which intercepts the K_f-line that represents the Mohr-Coulomb failure criteria. For undrained cyclic shear, the application of shear stresses to saturated soils causes the pore pressures to increase and the effective confining stress to decrease as shown in Fig. 7b. Cyclic shear can continue until the effective confining stress, p', reduces to the point where the applied shear stress, τ, intercepts the K_f-line as shown in Fig. 8. The value of effective confining stress at this point must be given by
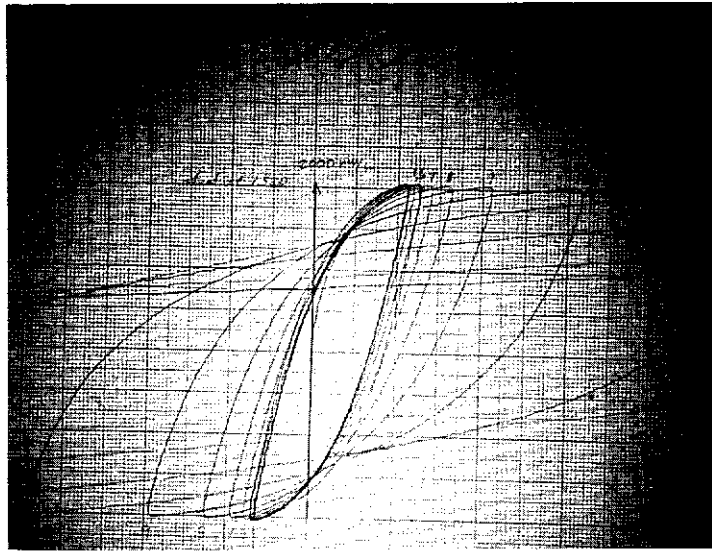
18

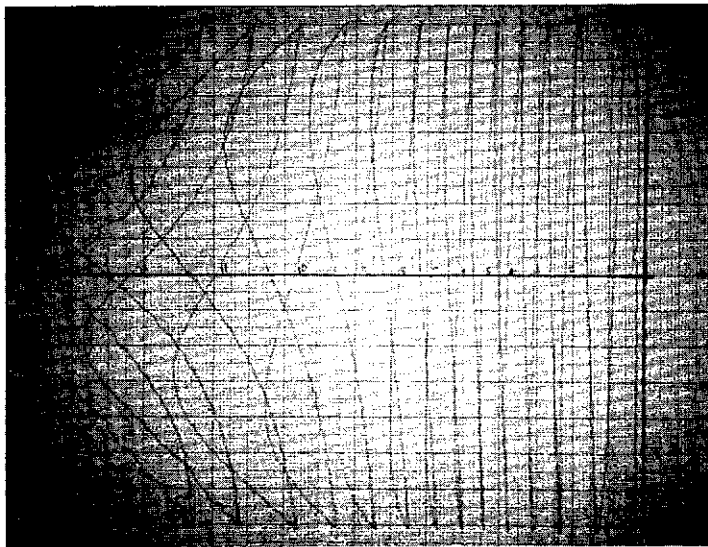Fig. 7a. Typical Shear Stress versus Shear Strain Results for Cyclic Shear

Fig. 7b. Typical Effective Stress Path Results for Undrained Cyclic Shear

Table III Undrained Cyclic Shear Test Results

Test No.	Soil	τ/τ_{max}	Freq. (Hz)	p' Fail. (Kg/cm^2)	Cycles to Fail.	Shear Strain @ Failure (Rad. x10^{-4})
1	Ottawa Sand	.100	50-40	.106	--	--
2	" "	.129	50-36	.131	7.5×10^6	--
3	" "	.840	0.1	.437	2.0	--
4	" "	.751	0.1	.767	115*	8.
5	" "	.467	52-16	.243	5,600*	7.8
6	" "	.468	52-33	.127	2.3×10^4	7.3
7	" "	.167	43-38	.087	--	--
8	" "	.207	44-16	.212	3×10^5	4.0
9	" "	.534	33-15	.145	2×10^4	3.5
10	" "	.191	49-42	.195	8×10^5	4.0
11	" "	.332	38-16	.172	5.4×10^5	3.5
12	" "	.449	0.1	.233	--	--
13	" "	.384	0.1	.200	13.5	39.5
14	" "	.389	0.1	.203	175	25.5
15	" "	.386	0.1	.394	12	19.4
16	" "	.550	0.1	.148	7	30.6
17	" "	.418	0.1	.112	41	31.8
18	" "	.459	0.1	.124	19	90.0
19	" "	.209	0.1	.420	3.6×10^5	1.4
20	" "	.454	0.1	.236	99	45.2
21	Reid Bed.	.708	0.1	.368	4	11.7
22	" "	.476	0.1	.248	82	7.5
23	" "	.700	0.1	.364	6	9.0
24	" "	.714	0.1	.727	1.5	19.6
25	" "	.551	0.1	.562	21	7.8
26	" "	.521	0.1	.531	42	10.0
27	" "	.360	0.1	.366	260	9.7
28	" "	.368	0.1	.375	221	8.0
29	" "	.418	0.1	.426	44	68.2
30	" "	.358	0.1	.365	100	21.4
31	" "	.465	0.1	.475	10	31.0
32	Monterey	--	0.1	--	--	--
33	"	.923	0.1	.480	1	26.2
34	"	.327	0.1	.166	565	62.7
35	"	.756	0.1	.393	5	9.1
36	"	.232	0.1	.238	--	--
37	"	1.00	0.1	.534	.25*	23.9
38	Granite	--	0.1	--	.25*	--

*Estimated from data.

Table III Cont'd Undrained Cyclic Shear Test Results

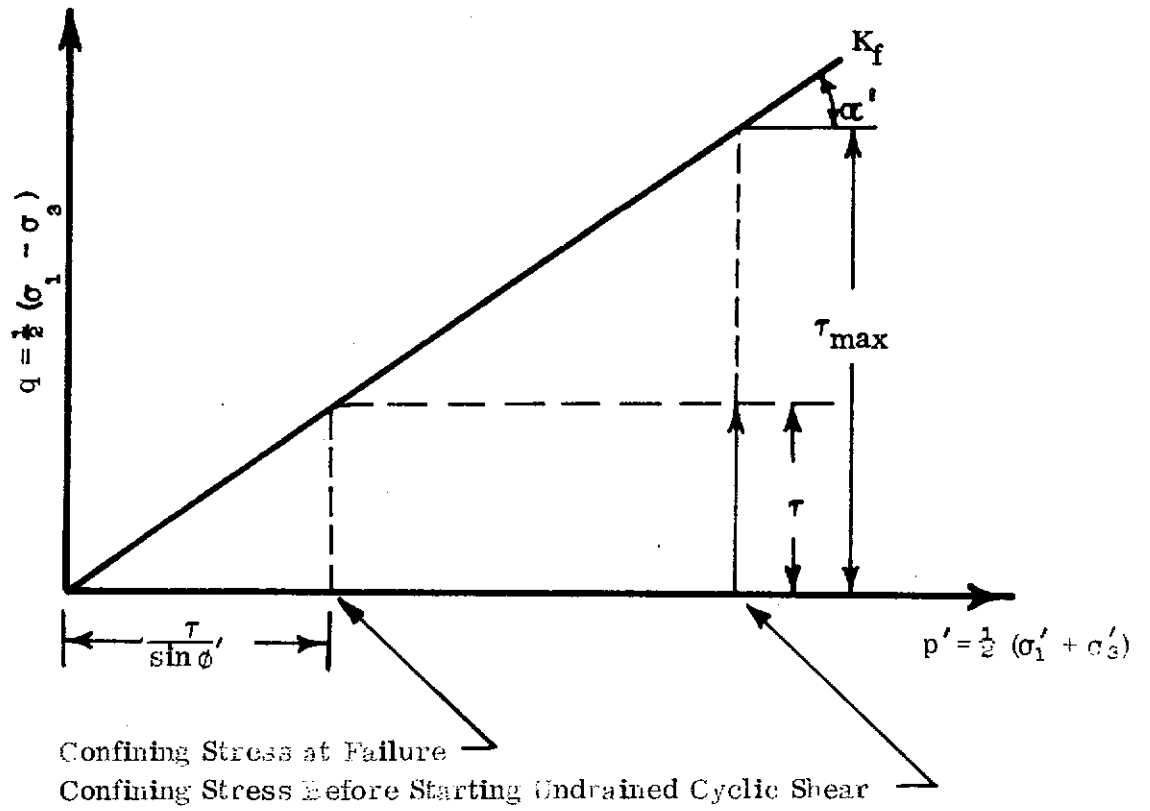| Test No.	Soil	τ/τ_{max}	Freq. (Hz)	p' Fail. (Kg/cm^2)	Cycles to Fail.	Shear Strain @ Failure (Rad. x 10^{-4})
39	Hawaii	.787	0.1	.409	1	47.8
40	"	--	0.1	--	--	--
41	"	.837	0.1	.435	1.5	39.9
42	"	.770	0.1	.400	3	27.7
43	"	.770	1.0	.399	15.	11.7

Fig. 8 Conditions for Failure Due to Undrained Cyclic Shear

$$p'\text{failure} = \frac{\tau}{\sin\phi'}$$

where ϕ' is the Mohr-Coulomb angle of shearing resistance $(\tan\alpha' = \sin\phi')$. Values of p'_{fail} are listed in Table III.

The number of cycles of undrained cyclic shear required to reduce the effective confining stress from the initial values to the value associated with failure are also given in Table III. These values are related to the initial value of τ/τ_{max} as can be seen from Fig. 9. The data with solid data points are for those tests where the cyclic shear was done at a frequency of 0.1Hz. The circled points are for those tests where cyclic shear was done first at a frequency of 0.1Hz for 1000 cycles and then the system switched over to resonance where the frequencies ranged from 16Hz to 52Hz. The point at 15 cycles to failure and moving can ordinate of 0.77 was a quasi-static test run at a frequency of 1 Hz. (Test No. 43). This test was identical in all respects to the previous test (Test No. 42) except in frequency of undrained cyclic shear. Increasing the frequency from 0.1Hz to 1 Hz increased the number of cycles to failure from 3 to 15 for this soil and initial conditions. The 1Hz rate of testing was the upper limit for the quasi-static capabilities of this apparatus and the test at this rate was extremely difficult to perform due to synchronizing problems among the three recorders being used. Any large scale testing program at rates faster than 0.5Hz would have to rely on an automated data acquisition system to acquire good quality data.

The solid curve drawn through the data points represents the average behavior for four sands and a wide variety of initial densities and confining stresses. Since 0.1Hz represents a practical lower bound in earthquake generated frequencies, this curve should give conservative results when used to predict the possibility of liquefaction for earthquake loadings. The curve may be described by the following equations.

$$N_f = 10^{[2.41-3.01(\tau/\tau_{max})]} \qquad 0.25 \leq N_f \leq 1$$

$$N_f = 10^{[1.76/(\tau/\tau_{max})-2.20]^{0.879}} \qquad 1 \leq N_f \leq 10^6$$

The next step in describing soil behavior during undrained cyclic shear is to define the effective confining stresses as a function of number of number of
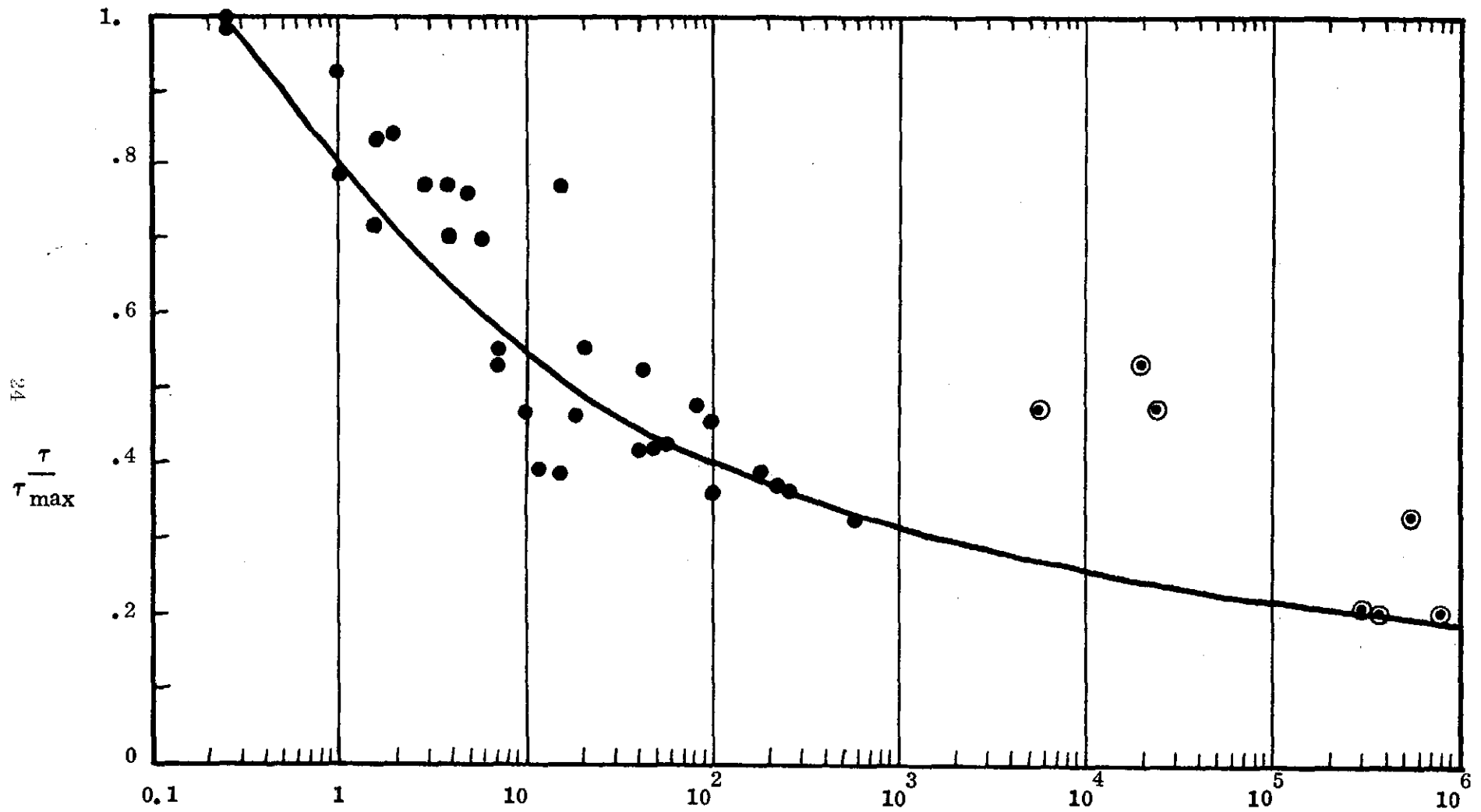
23

Fig. 9 Cycles of Undrained Cylic Shear for Failure

cycles of loading. Analysis of the data revealed that the decrease in confining stress was almost a linear function and that it was also primarily a function of the ratio τ/τ_{max}. All data were normalized by dividing by the initial values of effective confining stress. It was found that this ratio could be expressed by the following equation

$$\sigma_o'/\sigma_{oi}' = 1 - (1 - \tau/\tau_{max})(N/N_f)$$

where σ' is the effective confining stress at Nth cycle

σ_{oi}' is the effective confining stress before undrained cyclic shearing

N is the number of cycles of undrained cyclic shear

N_f is the number of cycles of undrained cyclic shear to produce failure.

Values of σ_o'/σ_{oi}' calculated by this equation are plotted in Fig. 10 versus measured values of σ_o'/σ_{oi}'.

Once confining stresses are known, it then becomes possible to estimate the values of shear modulus and shear damping. Equations developed by Hardin and Drnevich (6) were used for this. These equations were based on numerous tests on a variety of soils but were based on drained as opposed to undrained cycling. Use of the equations requires that a reference strain, γ_r, defined for each value of modulus or damping. The reference strain is given by

$$\gamma_r = \tau_{max}/G_{max}$$

where τ_{max} is the maximum drained shearing resistance for a given effective confining stress, and

G_{max} is the initial tangent shear modulus for that same effective confining stress.

For these tests, τ_{max} was calculated from

$$\tau_{max} = (\tau_{max}) \quad \sigma_o'/\sigma_{oi}'$$

where $(\tau_{max})_i$ was the value before the individual cyclic shearing and

σ_o'/σ_{oi}' is the confining pressure ratio for the point in question.

The Hardin-Drnevich equations also require the shear strain amplitude to determine shear modulus and shear damping. With all this information, a hyperbolic strain, γ_h, can be calculated from

$$\frac{\sigma_0{}'}{\sigma_{0i}{}'} = 1 - (1 - \tau/\tau_{max}) \ N/N_{fail.}$$

Calculated $\sigma_0{}' / \sigma_{0i}{}'$
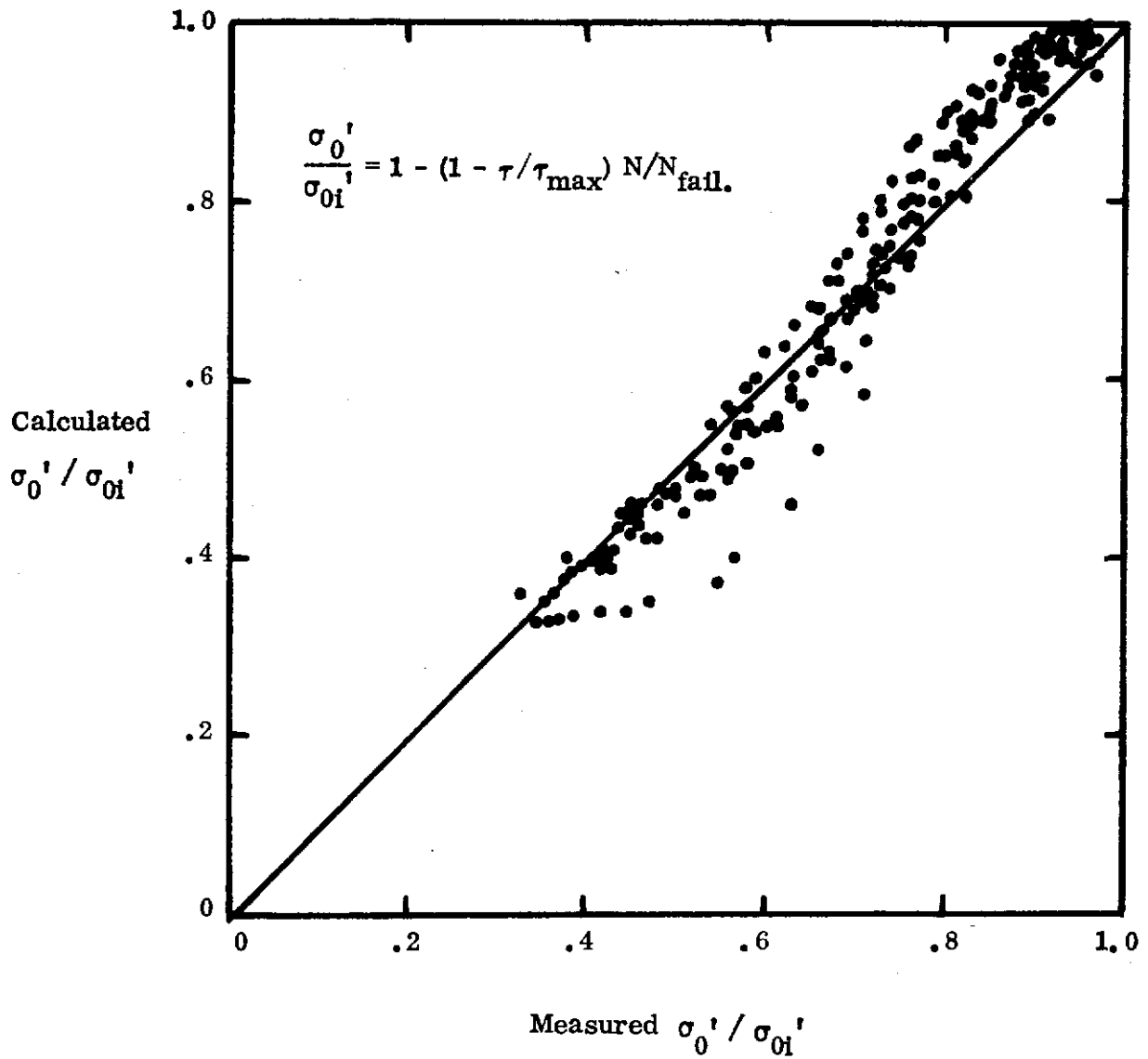
Measured $\sigma_0{}' / \sigma_{0i}{}'$

Fig. 10 Calculated versus Measured Effective
Confining Pressure Ratios

$$\gamma_h = \gamma/\gamma_r \ [1 + a \ \exp(-b\gamma/\gamma_r)]$$

where values of a and b for saturated sands are given in Table IV. Note that the values of a and b for shear modulus determination are different from those for shear damping determination. Finally, shear modulus and shear damping are given by

$$G = G_{max}/(1 + \gamma_h)$$

$$D = D_{max} \gamma_h/(1 + \gamma_h)$$

where D_{max} in percent is given by

$$D_{max} = 28 - 1.5 \log(N)$$

These equations were used to calculate shear modulus and damping values for the tests run in this program. The calculated shear moduli versus measured shear moduli are given in Fig. 11. It is obvious from the results that the Hardin-Drnevich equations for shear modulus also apply to undrained cyclic loadings.

The calculated values of shear damping are plotted versus the measured values in Fig. 12. Agreement for these data are not as good as for the modulus data. This is due in part to the difficulty in accurately measuring damping. Furthermore, the measured values are practically all larger than the calculated values. Part of the reason for this is due to the variable apparatus damping caused by the excitation motor and rotational motion measuring system. The calculated values would give lower, and thus conservative values for design purposes.

The procedures for estimating soil behavior for use in analysis and design will now be outlined. It is assumed that the soil profile has been defined and that geostatic stresses are known. It is also assumed that the earthquake characteristics are known and that the shear stress versus time record is available for any point in the soil profile. (An iterative procedure using the results to be calculated may have to be used to accurately obtain this record). This record is next converted to an equivalent number of shear stress cycles having an amplitude of 65 percent of the peak shear stress in the record according to the procedures developed by Seed and Idriss (11). A value of τ_{max} is needed before this shear stress can be

27

Table IV. Values of a and b for Calculation of Modulus and Damping for Clean Saturated Sands (Ref. Hardin and Drnevich (6)).

Modulus	Damping
a = -0.2 log N	a = 0.54 $(N^{-1/6})$ - 0.9
b = 0.16	b = 0.65 $(1 - N^{-1/12})$

Calculated values based on measured value of G_{max} and
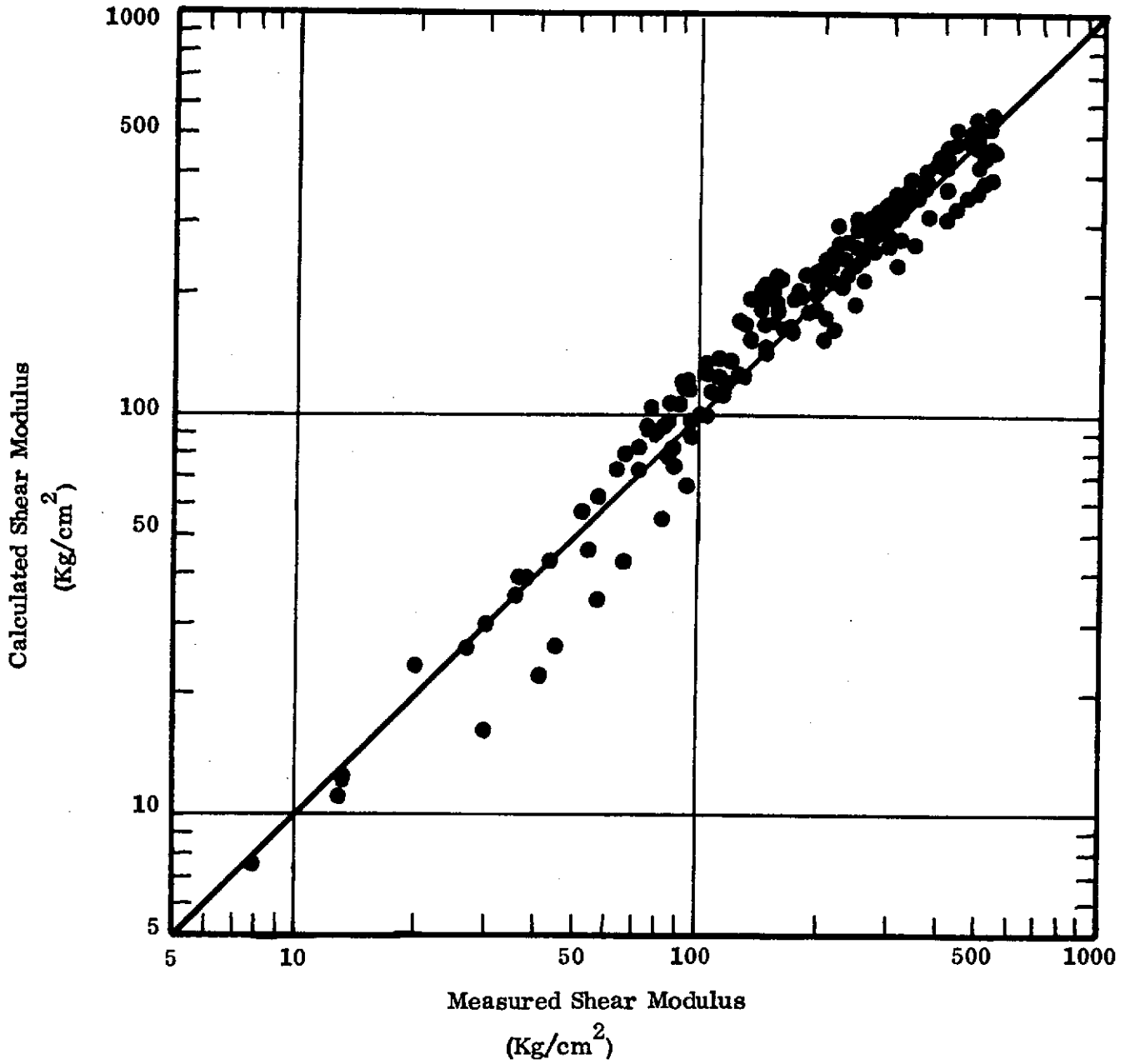Hardin-Drnevich equations.

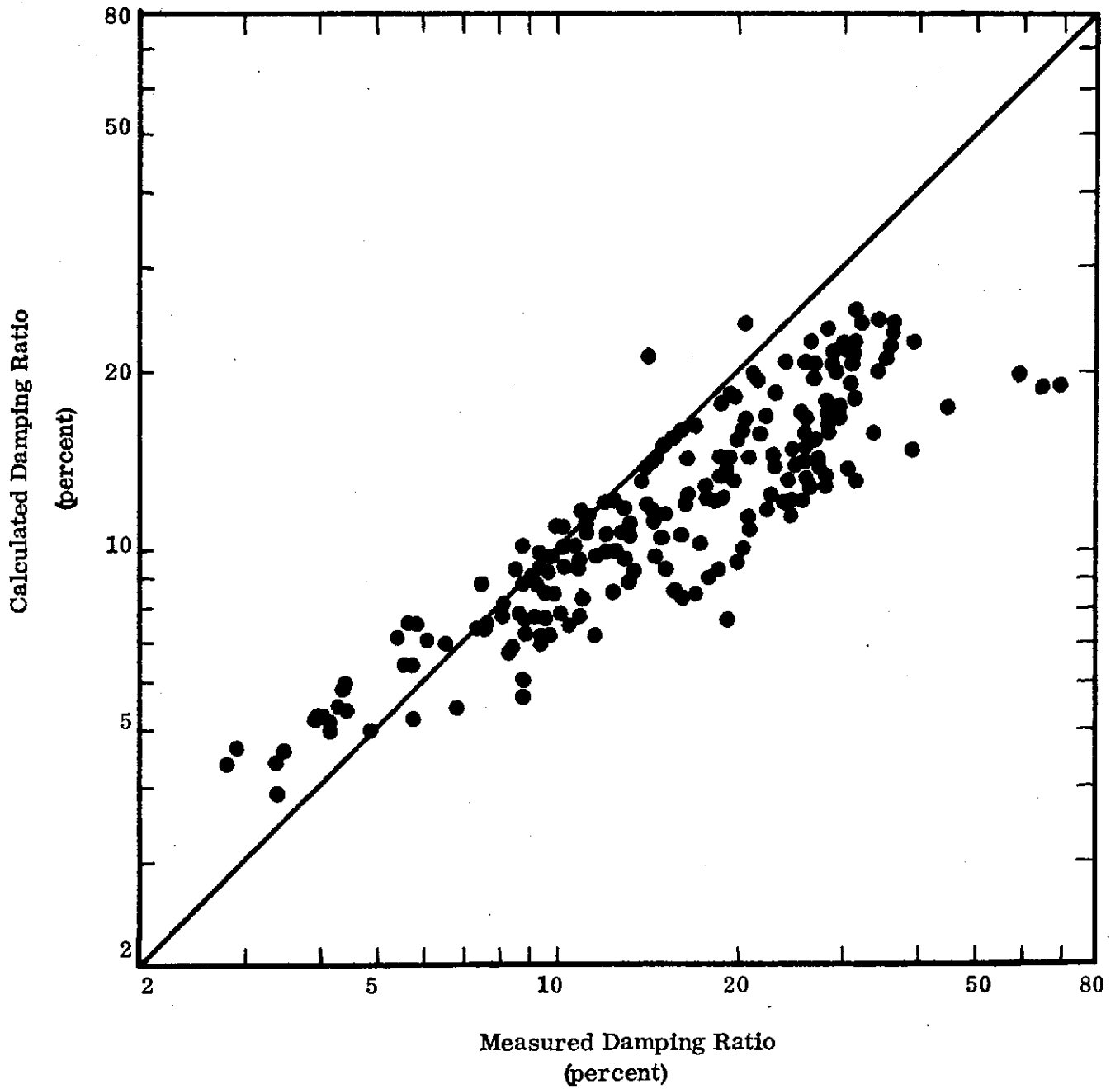Fig. 11 Calculated versus Measured Shear Moduli

Fig. 12 Calculated versus Measured Shear Damping

used and τ_{max} can be calculated from

$$\tau_{max} = \left\{ [1/2\,(1 + K_o)\,\sigma_v'\,\sin\phi' + c'\cos\phi']^2 \right.$$
$$\left. -[1/2\,(1 - K_o)\sigma_v']^2 \right\}^{1/2}$$

where K_o is the coefficient of earth pressure at rest

σ_v' is the vertical effective stress due to overburden

ϕ ' is the effective angle of shearing resistance

c' is the effective cohesion.

Now it is possible, by use of Fig. 9 to determine the number of cycles to failure, N_f, based on the value of τ/τ_{max}. If the equivalent number of cycles for the given earthquake exceeds N_f then a liquefaction failure will occur. For subfailure conditions, it is possible to determine the effective confining pressure at a given number of cycles from the equation used in Fig. 10. To use this figure, the value of σ_{oi}' is determined from the geostatic stresses by

$$\sigma_{oi}' = (1 + 2K_o)\,\sigma_v'/3$$

where K_o and σ_v' are as defined above.

A factor of safety against liquefaction failure for any number of cycles can be calculated from

$$F.S. = \frac{\sigma_o'\,\sin\phi'}{\tau}$$

where τ is the equivalent cyclic shear stress calculated for the given earthquake and

σ_o' is determined from Fig. 10.

If values of shear modulus and shear damping are desired, these may be calculated by means of the Hardin-Drnevich (6) equations. These equations require a number of parameters, all of which are known except the initial tangent shear modulus, G_{max}, and the shear strain amplitude, γ. The value of G_{max} is best determined by insitu seismic tests that measure the shear wave propagation velocity. Thus

$$G_{max} = \frac{\gamma_{soil}}{g}\,V_s^2$$

31

where γ_{soil} is the total unit weight of the soil

g is the acceleration of gravity

V_S is the shear wave propagation velocity.

In lieu of insitu seismic tests, G_{max} can be calculated from the Hardin Equation (6).

$$G_{max} (Kg/cm^2) = 326 (2.97-e)^2 (\sigma_o')^{1/2} /(1+e)$$

where e is the void ratio of the soil and

σ_o' is the mean effective confining stress in units of Kg/cm^2.

The shear strain amplitude may be estimated from

$$\gamma = \tau/(G_{max}(1-\tau/\tau_{max}))$$

After calculating the value of shear modulus, G, by the Hardin-Drnevich equations, a revised value of shear strain amplitude can be obtained from

$$\gamma = \tau/G$$

and this can be used in the Hardin-Drnevich equations to obtain an improved value of modulus.

Once the shear modulus has been obtained and the shear strain amplitude has been established, the Hardin-Drnevich equations can be used to calculate the shear damping.

CHAPTER IV

CONCLUSIONS

The objectives of this project were to define changes in effective confining pressure, shear modulus and shear damping for a variety of saturated sands due to cyclic shear where drainage from the soil was prevented. The results of forty-three tests were used to establish a curve relating the ratio of applied cyclic shear stress to maximum possible shear stress to the number of cycles required to produce liquefaction failure. Some data scatter existed and it was due to a number of causes among which are: difficulty in constructing uniform, hollow cylindrical specimens, inaccurate specimen density measurement, and problems associated with instrumentation. When all the data are considered, the resulting best fit curve gives reasonable results. It was found that cycling at a frequency of 0.1Hz caused liquefaction to occur in less cycles than did cycling at 1Hz or at resonance which was in a range of 15Hz to 50Hz.

Effective confining stresses reduced approximately linearly with number of undrained cycles. It was possible to fit all test data with a reasonably simple equation to describe the effective confining stress.

The equations developed by Hardin and Drnevich (6) for cyclic shear applied to saturated sands under drained conditions were found to apply to undrained conditions if the proper values of effective confining stress, initial tangent shear modulus, and maximum shear stress are used.

Finally, procedures for use of the findings of this research in determining the liquefaction potential of soil in place due to an earthquake were outlined. Furthermore, for subliquefaction conditions, procedures and equations were developed to calculate: factors of safety, shear modulus and shear damping. With this information it is now possible to analyze dams, earth fills and general soil profiles much more accurately for their response and behavior during earthquakes.

REFERENCES

1. , 1974 Annual Book of Standards, ASTM, Part 19, Designation D 2049-69, April 1974, pp. 252-260.

2. Drnevich, V. P., Effect of Strain History on the Dynamic Properties of Sand, thesis presented to the University of Michigan, at Ann Arbor, Michigan, in 1967, in partial fulfillment of the requirements for the degree of Doctor of Philosophy.

3. Drnevich, V. P., "Undrained Cyclic Shear of Saturated Sand," Jour. of the Soil Mechanics and Foundations Div., ASCE, Vol. 98, No. SM8, Proc. Paper 9134, August, 1972, pp. 807-825.

4. Hardin, B. O., "Suggested Method of Test for Shear Modulus and Damping of Soils by the Resonant Column," Special Procedures for Testing Soil and Rock for Engineering Purposes, ASTM, STP479, June 1970, pp. 516-529.

5. Hardin, B. O. and Drnevich, V. P., "Shear Modulus and Damping in Soils: Measurement and Parameter Effects," Jour. of the Soil Mechanics and Foundations Div., ASCE, Vol. 98, No. SM6, June 1972, pp. 603-624.

6. Hardin, B. O. and Drnevich, V. P., "Shear Modulus and Damping in Soils: Design Equations and Curves," Jour. of the Soil Mechanics and Foundations Div., ASCE, Vol. 98, No. SM7, July 1972, pp. 667-692.

7. Jent, J. P., "Description and Operation of a Torsion Apparatus for Soil Testing," Report submitted to Department of Civil Engineering, Univ. of Kentucky in partial fulfillment of the requirements for the degree of Master of Science in Civil Engineering, April, 1974.

8. Lambe, T. W., and Whitman, R. V., Soil Mechanics, John Wiley & Sons, New York, 1969, pp. 107-116.

9. Meyerhof, G. G., "Compaction of Sands and Bearing Capacity of Piles," Jour. of the Soil Mechanics and Foundations Div., ASCE, Vol. 85, No. SM6, Part 1, December, 1959, pp. 1-30.

10. Richart, F. E., Hall, J. R., Jr., and Woods, R. D., Vibrations of Soils

and Foundations, Prentice-Hall, Englewood Cliffs, New Jersey, 1970. 414 p.

11. Seed, H. B., and Idriss, I. M., "Simplified Procedure for Evaluating Soil Liquefaction Potential," Jour. of the Soil Mechanics and Foundations Div., ASCE, Vol. 97, No. SM9, September 1971, pp. 1249-1273.